[12] Robinson, G. D. and Drummond, A. J., "Some Recent Aircraft Measurements of the Absorption and Scattering of Solar Radiation by Atmospheric Aerosol," *Proceedings of the International Conference on Weather Modification*, AMS Boston, Mass., 1971, pp. 288–295.

[13] McLellan, A., "Global and Local Scale Satellite Surveillance of Atmospheric Pollution," *Proceedings of the Technical Program; Electro-Optical Systems Design Conference*, Industrial and Scientific Conference Management, Inc., Chicago, Ill., 1972, pp. 244–249.

[14] Darcey, R. J., "Meteorological Data Catalog for the Applications Technology Satellites, Part II," *The A.T.S. III User's Guide and Data Catalog*, Goddard Space Flight Center, Greenbelt, 1968, p. 353.

[15] Sundborg, A., "Local Climatological Studies of the Temperature Conditions in an Urban Area," *Tellus*, Vol. 2, 1950, pp. 221–232.

[16] Nader, J. S., ed., *Pilot Study of Ultraviolet Radiation in Los Angeles, October 1965*, U.S. Department of Health, Education, and Welfare, National Center for Air Pollution Control, Cincinnati, Ohio, 1967.

[17] McCormick R. A. and Baulch, D. M., "The Variation with Height of the Dust Loading Over a City as Determined from the Atmospheric Turbidity," *Journal of Air Pollution Control Association*, Vol. 12, 1962, pp. 492–496.

[18] Rasool, S. I. and Schneider, S. H., "Atmospheric Carbon Dioxide and Aerosols: Effects of Large Increases on Global Climate," *Science*, Vol. 173, 1971, pp. 138–141.

Striated Nozzle Flow with Small Radius of Curvature Ratio Throats

D. J. NORTON* AND R. E. WHITE†
Texas A&M University, College Station, Texas

Nomenclature

A,A_c = area, chamber area
c^* = characteristic velocity
C_p = specific heat, constant pressure
C_D = discharge coefficient
h,H_o = enthalpy, total enthalpy
$\dot{m}$ = mass flow rate
M = Mach number
n = curvature exponent
P,Po = static, total pressure
r,z = radial, axial coordinates
R,R_c = streamline, throat curvature
R_T = throat radius
T = temperature
u,w = radial, axial velocity
γ = isentropic exponent
ε_C = contraction ratio
ρ = density
ψ = streamline function

Subscripts and Superscripts

g,I = gas, injector
fu,ox = fuel, oxidizer
i = striation zone index
total = integrated total amount
1-D = one-dimensional
$()^\circ$ = reference quantity

Received May 1, 1973. This work was sponsored by NASA Johnson Spacecraft Center under Contract NAS 9-11658.

Index categories: Subsonic and Transonic Flow; Nozzle and Channel Flow.

* Assistant Professor, Aerospace Engineering. Member AIAA.

† Graduate Assistant, Aerospace Engineering. Student Member AIAA.

Introduction

In small rocket motors heat transfer can have a significant effect on engine efficiency as well as thermal protection requirements. A reduction in the heat-transfer coefficient can sometimes be accomplished by laminarization of the boundary layer using a highly convergent subsonic section and a small radius of curvature ratio throat.[1,2] In addition to a reduction in the heat-transfer coefficient, a decrease in nozzle surface area can be achieved. Further reductions in over-all heat transfer to the nozzle walls may be effected by use of barrier cooling. In the treatment of striated flow with throat radius of curvature effects no closed form relationship exists between the chamber pressure and the mass flow. This is due to variation of total enthalpy and velocity in the chamber due to striation as well as radial pressure gradients at the physical throat due to radius of curvature effects. Thus, choking for a given throat radius can only be described and identified (and the flow parameters determined) when coupled solutions between the throat and the chamber are employed. Even for unstriated nozzle flow, the solution for the two-dimensional flowfield with small radius of curvature ratio throats is difficult and time consuming.[3] When designing rocket motors a rapid means of estimating the performance of a motor with barrier cooling and for sharp throats is therefore desirable to permit the evaluation of potential designs.

Analysis

Since the throat solution is coupled to the chamber solution, it is also necessary to establish the relationship between the injection scheme and the throat. Figure 1a presents the flow regimes of interest in which mass, momentum, and energy

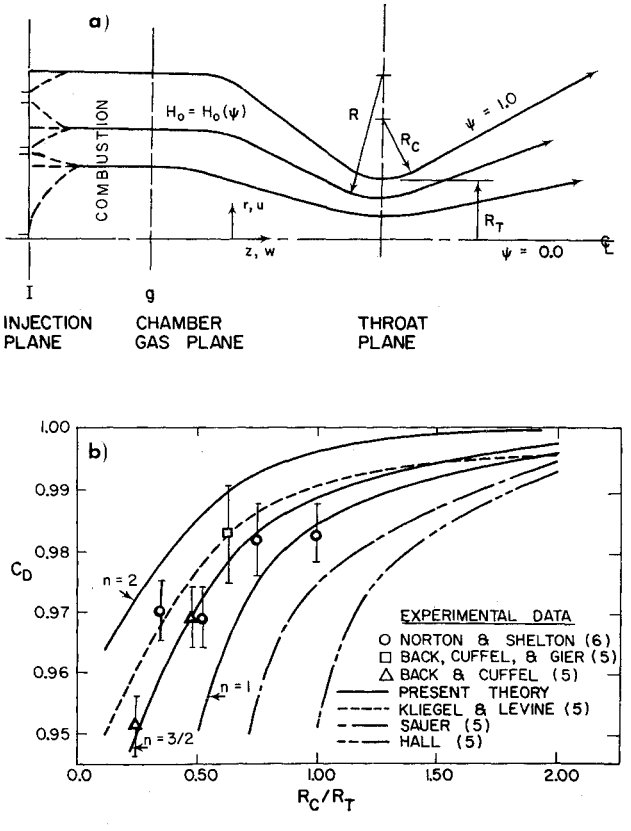

Fig. 1 a) Nozzle schematic and flow geometry; b) theoretical and experimental results for C_D vs R_C/R_T.

are conserved along streamlines. The flow in the chamber is assumed to be one-dimensional. In general, the injector characteristics are specified. Chemical reaction (combustion) occurs between the injector face (*I-I*) and some arbitrary downstream plane where the products are gaseous (*g-g*). The conservation equations of mass, momentum, and energy of each chamber flow zone for adiabatic flow are

$$(\rho_I w_I A_I)_{fu_i} + (\rho_I w_I A_I)_{ox_i} = \dot{m}_i = \rho_{g_i} w_{g_i} A_{g_i} \quad (1)$$

$$(\dot{m}_I w_I)_{fu_i} + (\dot{m}_I w_I)_{ox_i} + A_{g_i} P_I = P_g A_{g_i} + \dot{m}_i w_{g_i} \quad (2)$$

$$(H_{o_I})_i = (H_{o_g})_i = h_{g_i} + w_{g_i}/2 \quad (3)$$

where

$$h_{g_i} = \int_{T^\circ}^{T_{g_i}} (C_{p_g})_i dT + h_{g_i}{}^\circ$$

In addition, three other constraints that appear necessary and consistent with the one-dimensional assumption

$$P_{I_i} = P_I, \qquad P_{g_i} = P_g, \qquad \sum_i A_{g_i} = A_c \quad (4)$$

Now if the injector parameters are specified, a solution for the area, velocity, temperature, and chemical constituency of each chamber zone can be determined.

The momentum and mass equations together with the requirement that energy be conserved in stream tubes defines the flow at the throat. The radial momentum equation for axisymmetric inviscid flow without swirl is

$$\partial P/\partial r = \rho[u \partial u/\partial r + w\, \partial u/\partial z] \quad (5)$$

At the throat plane we expect that the effect of radial velocity will be small since it must be zero at the wall and centerline. Since on a streamline $dr/dz = u/w$, then on the throat plane between the circular arc throat wall and the centerline

$$dP/dr = \rho w\, du/dz = -\rho w^2\, d^2r/dz^2 = -\rho w^2/R \quad (6)$$

In this equation, R refers to the radius of curvature of the streamlines at the throat. The equation for conservation of mass and the energy equation when $u \simeq 0$ are

$$d\psi/dr = d\dot{m}/dr(1/\dot{m}_{\text{total}}) = 2\pi r \rho w/\dot{m}_{\text{total}} \quad (7)$$

$$w^2 = 2(H_o - h) \quad (8)$$

Applying Eq. (8) to Eqs. (6) and (7) results in a set of two nonlinear ordinary differential equations. The solution of these equations can be obtained at the throat providing H_o, h, R, and ρ can be specified as functions of ψ and P. It remains only to specify a relationship for R to close the formulation at the throat plane. It is clear from experimental and analytical studies that the main functional form for R should be $R = R(R_C, R_T, r)$. This formulation for R neglects effects due to inlet geometry between the chamber and the throat region; however, experimental evidence indicates this to be a minor variation except for nozzle contraction angles near 90° and/or for $R_C/R_T \simeq 0$ (Refs. 4–6). The appropriate boundary conditions for R regardless of striation effects are

$$R = R_C \quad \text{at} \quad r = R_T \qquad \text{and} \qquad R \to \infty \quad \text{as} \quad r \to 0$$

A plausible form for R which satisfies these conditions for n greater than zero is

$$R = R_C \left[\frac{R_T(1 + R_C/r) - r}{R_C}\right]^n \quad (9)$$

Figure 1b presents a number of calculations for the discharge coefficient C_D with respect to R_C/R_T for various values of n. Based on these results a value of $n = \frac{3}{2}$ is indicated. The representation chosen for R can be further evaluated by comparing results for the variation of throat plane Mach number and static to chamber pressure as a function of radius presented in Fig. 2. Results compare favorably to the data taken by Cuffel, Back, and Massier.[4] Equations (6) and (7) thus comprise the necessary governing equations at the throat since $H_o = H_o(\psi)$, $h = h(P, \psi)$, $\rho = \rho(P, \psi)$. $H_o(\psi)$ is determined in the chamber solution, while the relationship for h and ρ as a function of P and ψ depends on the type of flow to be considered. To initiate the throat solution, a centerline pressure must be chosen. The centerline pressure which yields the minimum wall radius identifies the throat plane. A solution is achieved when the computed throat radius matches the prescribed throat radius. Iteration between the chamber and the throat plane determines the compatible chamber solution which identifies choking of the flow for the desired geometry and fixed injection parameters.

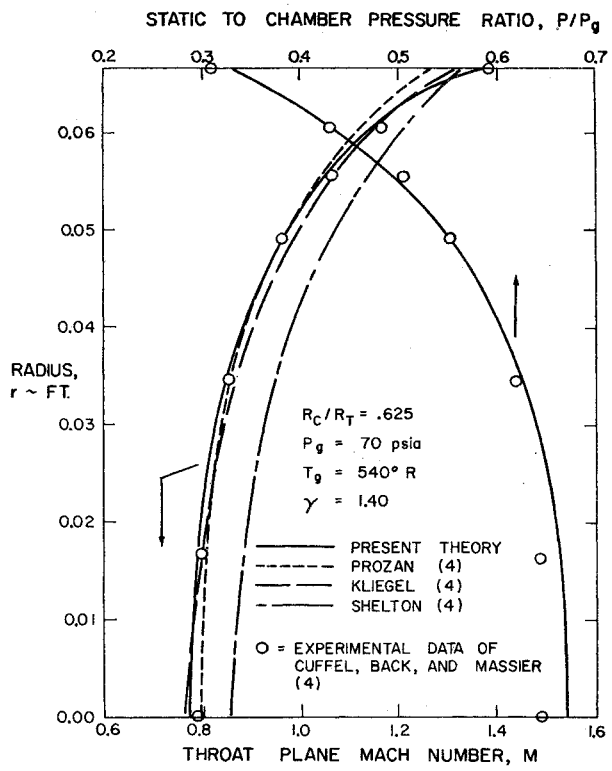

Fig. 2 Mach number and pressure at the throat plane.

Results

The effects of striated flow in nozzles with small radius of curvature throats has been investigated. Several types of flows were investigated: 1) frozen composition, calorically perfect, striated flow; 2) frozen composition, striated flow; 3) equilibrium, striated flow; and 4) frozen composition, calorically perfect, fully mixed flow. The first three types are for striated flow in which zones remain discrete. The last type was chosen for comparison to determine the maximum effects of mixing on the over-all performance of the motor.

Figure 3 presents a typical result for frozen, calorically perfect flow involving four zones of varying O/F ratio for an H_2/O_2 system. The throat solution presented is for the pressure and Mach number with several R_C/R_T. The pressure tends to low values at the wall for low R_C/R_T. The Mach number exhibits the opposite trend, however this curve is discontinuous across the zone interfaces due to step changes in the chemistry typical for no mixing.

Two performance parameters were used to evaluate the effects of striation and R_C/R_T.

$$C_D = \sum_i C_{D_i} = 2\pi \int_0^{R_T} \rho w r dr/\dot{m}_{\text{total}_{1-D}} \quad (10)$$

$$c^* = \frac{\pi R_T{}^2}{C_D{}^2 \dot{m}_{\text{total}_{1-D}}} \sum_i P o_{g_i} C_{D_i} \quad (11)$$

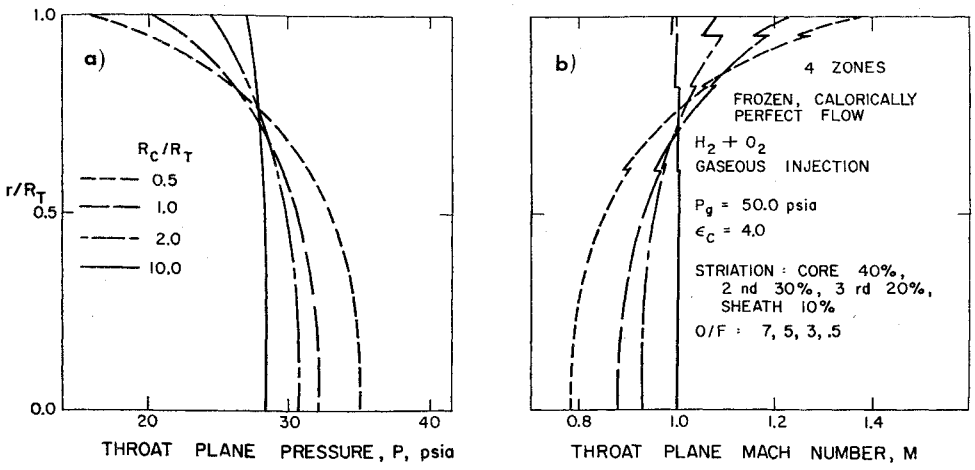

Fig. 3 Pressure and Mach number at the throat plane for 4 zones.

These parameters are useful in this study since no consideration to the extent of expansion of the nozzle is included. It can be seen that c^* is inversely related to C_D if the stagnation pressures of each zone are the same. This relationship is not necessarily true with striation, however, since the injection characteristics and chemistry may vary greatly from one zone to the next.

Figure 4a shows the variations of C_D with the cooling mass ratio. Several types of flow situations are considered. The fully mixed flow case occurs when the striated chamber flow becomes fully mixed before reaching the throat. The effect of this mixing is to reduce the variation of C_D with cooling mass ratio. In Figure 4b a H_2/O_2 propellant combination with a core $O/F = 7.0$ and a sheath $O/F = 0.0$ shows an improved discharge coefficient for 20% striation over unstriated flow. However, for a N_2H_4/N_2O_4 combination, the unstriated flow discharge coefficient is greater than the striated flow discharge coefficient. The results shown in Fig. 4b employ thermochemical data determined for a chamber static pressure of 200 psia and constant total enthalpy. The significance of Fig. 4b is that for striated flow using N_2H_4/N_2O_4 propellants less throat is required to accommodate the N_2H_4 barrier than is required for the H_2/O_2 propellant combinations using H_2 as a barrier for the same cooling mass ratio.

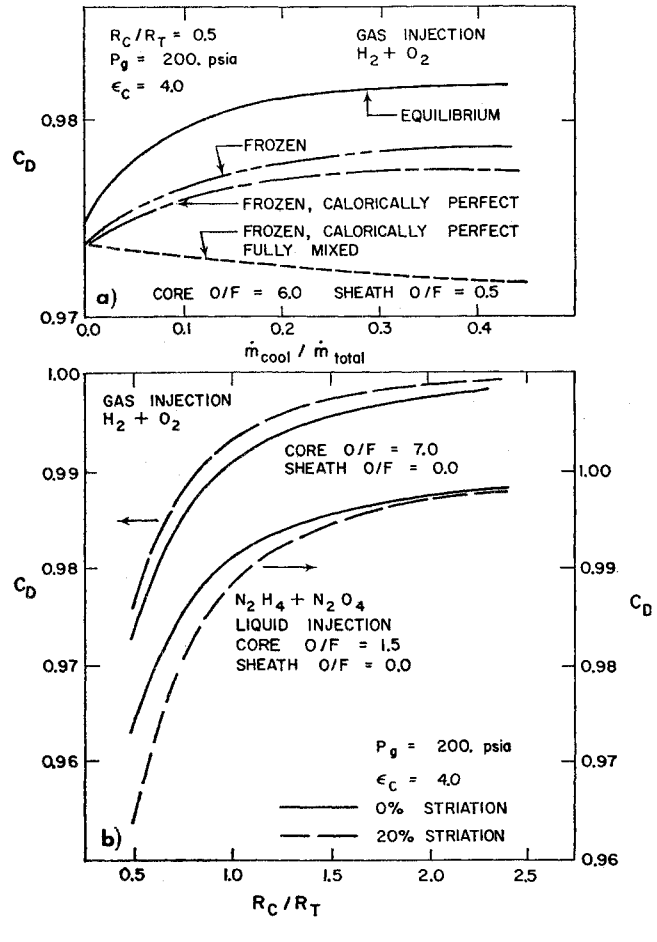

Fig. 4 a) C_D as a function of flow type and cooling; b) C_D as a function of R_C/R_T.

Conclusions

The theory presented here permits an extension of one-dimensional techniques for compressible striated nozzle flow with low radius of curvature ratio, circular arc throats. The throat plane solution approximates the two-dimensional axisymmetric flowfield and has successfully been used for analyzing the throat plane in converging-diverging type nozzles with striated flow for R_C/R_T down to 0.25. By coupling the chamber and throat plane solutions, chamber and throat plane spatial distributions of velocity and other thermodynamic parameters are uniquely determined for specified geometry. Results agree favorably with experimental data and results of other computational methods, especially in predicting C_D. The dependence of C_D is primarily on the radial pressure gradient, the adiabatic or isentropic coefficient, and the amount of mass in each flow zone.

Studies have yielded no general parameter combination which correlates striated to unstriated flow discharge coefficient without knowledge of the results of the throat plane solution. There is, however, a significant effect due to specific heat ratios in striated flow; stagnation temperatures and molecular weights have only a secondary effect on discharge coefficient.

References

[1] Back, L. H., Cuffel, R. F., and Massier, P. F., "Laminarization of a Turbulent Boundary Layer in Nozzle Flow," *AIAA Journal*, Vol. 7, No. 4, April 1969, pp. 730–733.

[2] Back, L. H. and Seban, P. A., "Flow and Heat Transfer in a Turbulent Boundary Layer with Large Acceleration Parameter," *Proceedings of the Heat Transfer Fluid Mechanics Institute*, 1967, pp. 410–426.

[3] Norton, D. J., "Subsonic, Transonic, and Supersonic Nozzle by the Inverse Technique," *Journal of Spacecraft and Rockets*, Vol. 9, No. 6, June 1972, pp. 457–459.

[4] Cuffel, R. F., Back, L. H., and Massier, P. F., "Transonic Flowfield in a Supersonic Nozzle with Small Throat Radius of Curvature," *AIAA Journal*, Vol. 7, No .7, July 1969, pp. 1364–1366.

[5] Back, L. H. and Cuffel, R. F., "Flow Coefficients for Supersonic Nozzles with Comparatively Small Radius of Curvature Throats," *Journal of Spacecraft and Rockets*, Vol. 8, No. 2, Feb. 1971, pp. 196–198.

[6] Norton, D. J. and Shelton, S., "Performance of Rocket Nozzles with Low Radius of Curvature Ratios," Space Programs Summary 37-55, Vol. III, Feb. 1969, Jet Propulsion Lab., Pasadena, Calif., pp. 167–169.

[7] Norton, D. J. and White, E., "Analytical Study of Striated Nozzle Flow with Small Radius of Curvature Ratio Throats," TEES-1092-TR-72-01, Aug. 1972, Texas A&M Univ., College Station, Texas.

Aerodynamic Force Measurement on Caret and Delta Wings at High Incidence

G. T. COLEMAN*

Imperial College of Science and Technology
London, England

1. Introduction

THE space shuttle program has focused attention on high lift re-entry vehicles such as flat-bottom delta wing configurations. The caret wing is also of interest because of its higher lift coefficient in comparison with the delta, due to the containment of a two-dimensional shock at its design incidence and the associated lack of flow spillage (assuming that heating considerations do not dictate blunted leading edges). The advantage of the caret wing in cruising flight was shown by Opatowski,[1] but there was a lack of information on its behavior under re-entry conditions until Rao[2] performed tests at $M = 12.2$ in the Imperial College No. 1 Gun Tunnel. These tests suffered from the effects of tunnel blockage and were repeated by Carr[3] with more success. The investigation described herein was conducted in the larger Imperial College No. 2 Gun Tunnel at $M = 9$ using the same models and balance. The results provide further insight into the behavior of lifting re-entry configurations at high angles of incidence.

2. Experimental Details

The tests were made using a three component force balance in the Imperial College No. 2 Gun Tunnel[4] which uses nitrogen as the test gas. The models (Fig. 1) had a preset angle of 30° between the balance sting and the windward surface and windward ridgeline, respectively, for the flat delta and caret wing.

3. Results and Discussion

Measurements of normal and axial forces and pitching moment were taken for both the flat bottom delta and caret wing model in the incidence range $30° \leqslant \alpha \leqslant 60°$, where α is the angle between the flow direction and the windward surface or windward ridgeline, respectively, for the flat delta and caret wing. The upper limit (60°) is higher than in previous tests. The test conditions are given in Table 1, where the subscript o, w, ∞ refer to reservoir, wall, and freestream conditions, respectively, and L' is the center chordlength of the models.

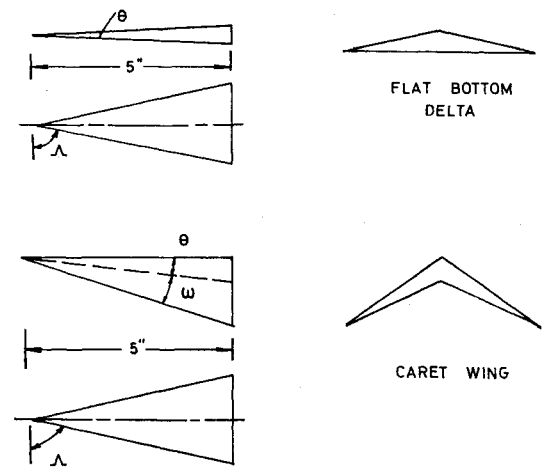

MODEL	Λ	θ	ω
FLAT DELTA	75°	6°	–
CARET WING	75°	6°	10°

Fig. 1 Details of the models.

Table 1 Test conditions

M_∞	Re_∞/in.	T_o °K	T_w °K	T_∞ °K	$Re_{L'}$
8.96	0.31×10^6	1070	295	65.5	1.55×10^6

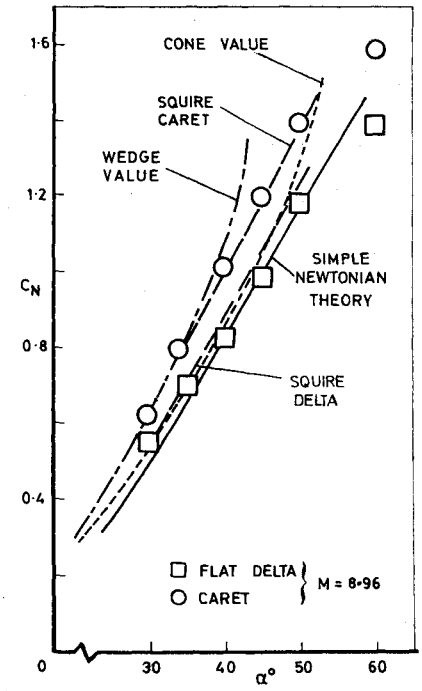

Fig. 2 Normal force coefficients for the flat delta and caret wing models.

Received May 9, 1973; revision received June 22, 1973.
Index category: Entry Vehicle Dynamics and Control.

* Research Assistant, Department of Aeronautics.